

RESEARCH ARTICLE | AUGUST 25 2023

Modification to a testing assembly to enable strain-life measurements in pressurized hydrogen gas

P. E. Bradley  ; M. L. Martin ; M. J. Connolly; R. L. Amaro; D. S. Lauria ; A. J. Slifka 



Rev Sci Instrum 94, 083906 (2023)

<https://doi.org/10.1063/5.0131798>



View
Online



Export
Citation

CrossMark

Articles You May Be Interested In

Hydrogen embrittlement in ferritic steels

Applied Physics Reviews (October 2020)

The Morlet wavelet transform for reducing fatigue testing time of an automotive suspension signal

AIP Conference Proceedings (July 2018)

Modification to a testing assembly to enable strain-life measurements in pressurized hydrogen gas

Cite as: *Rev. Sci. Instrum.* **94**, 083906 (2023); doi: [10.1063/5.0131798](https://doi.org/10.1063/5.0131798)

Submitted: 24 October 2022 • Accepted: 5 August 2023 •

Published Online: 25 August 2023



View Online



Export Citation



CrossMark

P. E. Bradley,^{1,a)}  M. L. Martin,¹  M. J. Connolly,¹ R. L. Amaro,² D. S. Lauria,¹  and A. J. Slifka¹ 

AFFILIATIONS

¹National Institute of Standards and Technology, Boulder, Colorado 80305, USA

²Advanced Materials Testing & Technologies, Cropwell, New Jersey 35054, USA

^{a)}Author to whom correspondence should be addressed: peter.bradley@nist.gov

ABSTRACT

Strain-controlled fully reversed fatigue testing, or strain-life testing, provides critical information on material lifetime and damage response. Strain-life data in hydrogen gas environments is missing in the literature and could provide valuable insights into hydrogen effects on the mechanical response of metals such as steel. We adapted existing hydrogen-gas-environment mechanical-testing equipment, which had been designed only for tensile loads, to accommodate the large compressive loads needed to perform strain-life testing. The considerations of these adaptations are discussed. Successful strain-life testing data were acquired from a 4130 pressure vessel steel.

Published by AIP Publishing. <https://doi.org/10.1063/5.0131798>

INTRODUCTION

Strain-controlled and force-controlled testing methods are used to elucidate the effects of loading and environmental conditions on material failure. Specifically, strain-controlled testing is traditionally used to probe a material's low cycle fatigue damage response (e.g., under 100 000 cycles), and stress-controlled testing is of primary value when interested in a material's high cycle fatigue damage response.^{1,2} While stress-controlled test data provide information about specimen separation, strain-controlled test data provide information about the onset of crack initiation as well as the material's load-history-dependent response evolution. Both testing methodologies are critical when considering the design and engineering of piping, pipelines, pressure vessels, and fittings/valves intended to be used in support of a future gaseous hydrogen infrastructure. Examining the mechanical response of a material in hydrogen and comparing that to the mechanical response in the air can be used to probe the mechanistic differences manifesting in the material between hydrogen and air environments. For many steels, and in particular ferritic steels, fatigue lifetimes are drastically reduced in hydrogen.³⁻⁹

At the National Institute of Standards and Technology (NIST) Boulder, Colorado campus, we have a laboratory specifically set up for mechanical properties testing in a high-pressure hydrogen gas

atmosphere using purpose-designed chambers containing the atmosphere around the sample and a portion of the load train of the testing machine. This setup has been used for tensile testing, fracture toughness testing, and fatigue crack growth rate testing;¹⁰⁻¹² loading in compression has not been a component of previous testing runs. We have modified an existing chamber and experimental setup for fully reversed measurements of the strain-life of materials in pressurized hydrogen gas. Our primary interest is the damage response of pressure vessel and pipeline steels in hydrogen environments. The chamber was designed for tensile loading only,¹³ but we required fully reversed loading for strain-life testing. We discuss the modifications and the reasoning behind them.

MEASUREMENT REQUIREMENTS AND CHALLENGES

Strain-life testing is the strain-controlled fully reversed loading of a smooth tensile bar until failure. The applied strain amplitude is varied to determine the lifetime as a function of the strain amplitude. During strain-life testing, the material's response is hysteretic, and hardening or softening may occur, depending upon the material. Example data are shown in Fig. 1(a). The test starts with a tensile pull, similar to a tensile test, until the maximum positive strain amplitude is reached, then the strain is released in a controlled

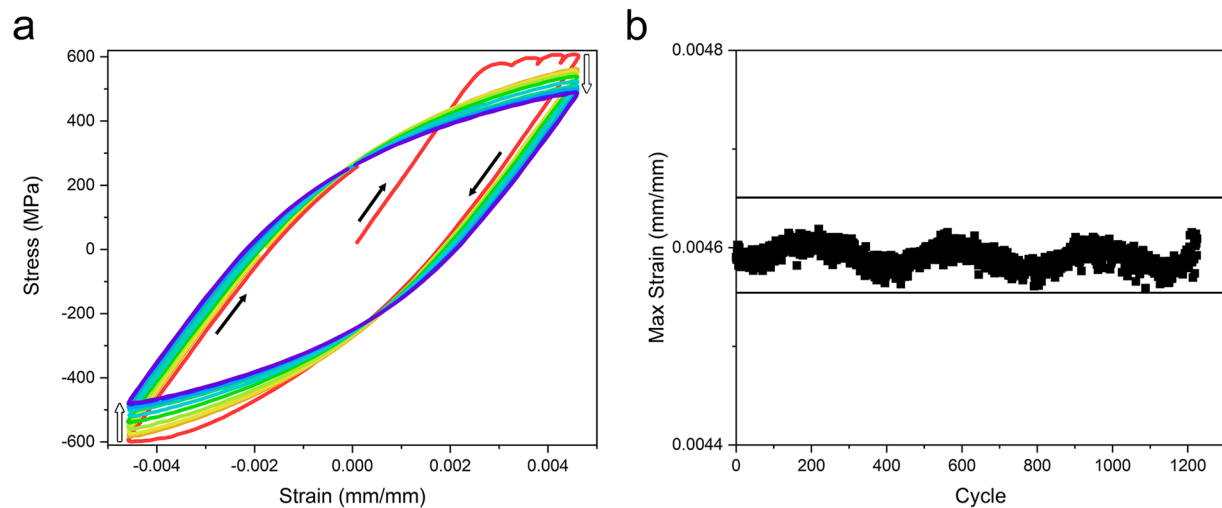


FIG. 1. (a) Plot showing data from a typical strain-life test in hydrogen. Data progress from the center (red) clockwise through the progressively cooler colors to blue. The decrease in the magnitude of the curves (indicated by the white arrows) is due to softening of the material as it fatigues. The first tensile pull displays ratcheting behavior. (b) Plot of maximum strain as a function of cycles. Strain control limits of 1% are plotted. Note that the measured maximum strain for each cycle does fall within these limits, such that the test is valid according to ASTM E606.¹⁴

fashion and the strain cycles toward compression, stopping at the negative strain amplitude, and the hysteretic behavior of the material is observed. This particular material displayed softening: the maximum and minimum stresses that the material can hold decrease with cycling. The softening is initially rather rapid, then stabilizes with further cycling. The process continues until a crack nucleates and the sample fails. The amount of plastic behavior, and, therefore, the shape of the hysteresis curve and the degree of softening of the material, will be dependent on the applied strain amplitude, with higher strain amplitudes resulting in greater amounts of plasticity and a wider hysteresis loop.

To achieve strain-life tests, the system must be able to apply both tensile and compressive strains/loads, must maintain tight control of the applied strain, must stay well aligned during the entirety of the process, and the sample design must ensure that fracture occurs within the gage length where the strain is measured. The measurement requirements for strain-life testing can be found in ASTM E606.¹⁴ This standard calls for minimization of backlash, limitation of maximum bending strains to less than 5% of the lowest strain range imposed during testing, and repeatable control of strain to within 1% of the minimum and maximum limits. This last feature is shown in Fig. 1(b).

For testing in pressurized hydrogen gas, these conditions must be met while somehow containing the hydrogen environment around the sample. Our laboratory uses a chamber, described previously,¹³ which surrounds the sample as well as a part of the load train. Prior to this study on strain-life, the chamber had only been used for tensile loading: any fatigue tests were generally run at $R > 0$ such that there was no compressive component to the applied load. Strain-life testing in hydrogen gas adds complications in transferring the tensile and compressive loads while maintaining the pressurized environment. The environment used was at least 99.9995% pure

hydrogen gas, typically at 18 MPa (2600 psi), at room temperature. In-air tests were run both with and without the presence of the chamber, with more recent tests maintaining the chamber in place with atmospheric pressure air at room temperature, to maintain similar alignment conditions for the in-air tests. We get fewer misaligned tests with the chamber in place, and successful tests with the chamber are indistinguishable from successful tests without the chamber.

The test was controlled for total axial strain amplitude, with a strain-ratio (R_ϵ) of -1 (fully reversed strain). Instead of a triangular waveform, which is preferred in the standard, a sinusoidal waveform was used for all tests because it provides a tighter control (typically better than 0.5%) over the entire strain cycle when testing in pressurized hydrogen gas. These tests were performed inside a chamber that has seals that can induce a significant frictional load on the actuator rod and may vary over time. The use of a waveform that provided better control was necessary to maintain tight strain accuracy under those conditions. All tests in pressurized hydrogen gas were done at a constant strain rate of 0.002 s^{-1} so that the highest test frequency was 1 Hz. (Frequency is the strain rate divided by the strain amplitude—the smallest amplitude tests will have the highest frequency.) This is the highest frequency at which hydrogen effects can be reliably captured in fatigue before frequency effects are dominant.^{12,15}

To maintain strain control throughout the test, and maintain a valid test, certain conditions need to be met. Strain amplitude is controlled to within 1% of the specified maximum and minimum. For instance, 0.0046 strain amplitude requires control between ± 0.004554 and ± 0.00465 strain, see Fig. 1(b). To achieve this strain amplitude, high compressive and tensile loads must be properly transferred to the sample. Part of achieving this involves minimizing bending, which could reduce the effective transfer of strain during

compression, as well as damage the sample and the equipment. This requires high lateral stiffness along the entire assembly. In addition, backlash must be minimized to prevent damage to the equipment and loss of hydrogen gas.

The ASTM E606 standard stipulates that bending strain be less than 5% of the maximum axial strain range within the gage length of the sample. Note 7 in the E606 standard discusses this allowance.¹⁴ However, the sample is not the only place where bending can cause problems, especially during the compression portion of the cycle. Care must be taken to ensure a minimum of deflection along the entire assembly.

To minimize backlash and provide lateral stiffness, we replaced our default pinned clevis with a custom-made compression clevis. The pinned clevis, Fig. 2(a), does not have the lateral stiffness for large compressive loads and the pin is generally too loose for fully reversed loading. The compression clevis uses eight bolts on two flanges to press the pull rod to the actuator rod of the load frame, eliminating any backlash at that point. The bolts are

3/4-10 size (diameter = 1.9 cm) and can easily be torqued to provide compression between the pull rod [the bottom in Fig. 2(b)] and the actuator rod [the top in Fig. 2(b)] even at the largest tensile loads encountered (24 kN) in our series of strain-life tests. The plates of the clevis are kept parallel by the use of four precision cylindrical aluminum spacers on four alternating bolts.

Other connection points that could have backlash include the point where the internal load cell connects to the inside of the lower end cap of the test vessel, where the lower specimen grip connects to the internal load cell, the button-head specimen connections to the specimen grips, and the upper specimen grip connection to the pull rod. All of these are shown, highlighted, in Fig. 3. These connections can all be firmly tightened except for the upper specimen grip connection to the pull rod, which is left slightly backed off from being firmly tightened. If that connection is too tight at the end of a test, the extensometers and associated wiring will be twisted and damaged. This “slack” results in a slight decrease in linear stiffness

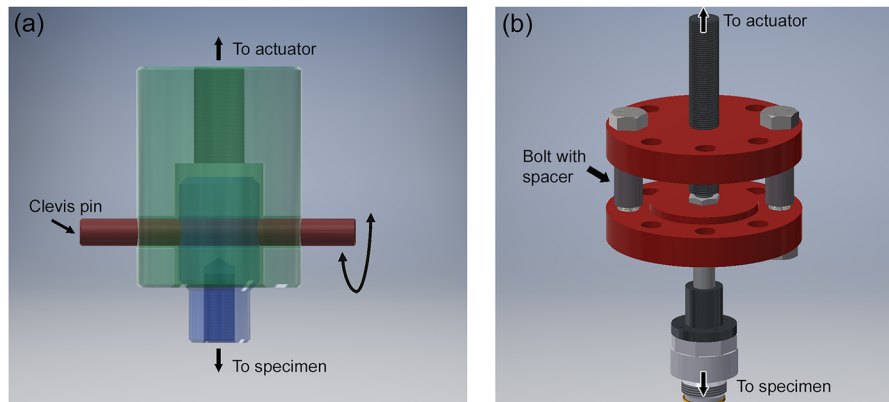


FIG. 2. (a) Drawing of an example clevis and pin connector for mechanical testing. (b) Drawing of the custom compression clevis that uses eight 3/4-10 bolts and four precision aluminum spacers to assure that plates remain parallel. Only two bolts and spacers are shown in the diagram for clarity.

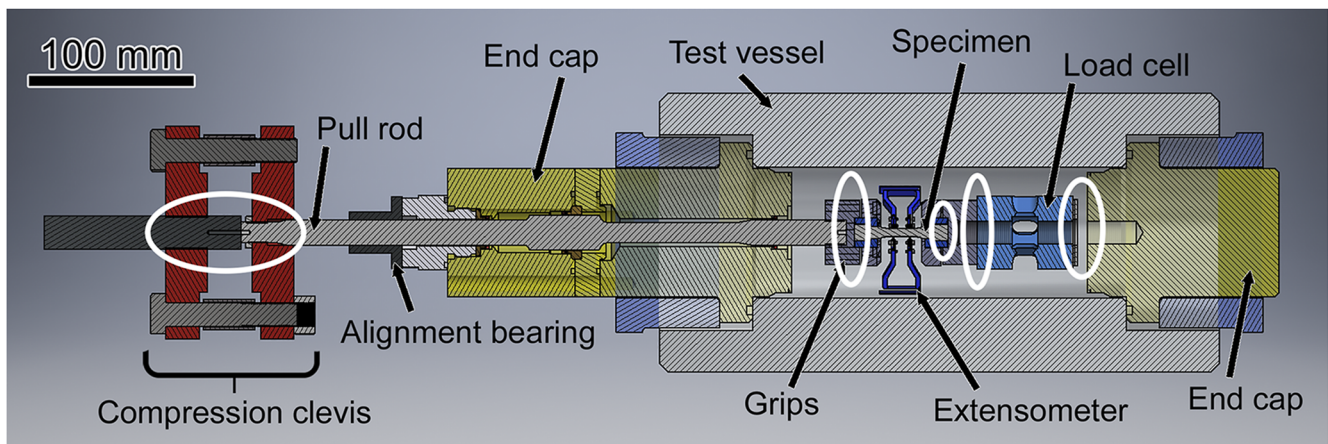


FIG. 3. Drawing of the test vessel and associated parts for strain-life testing in pressurized hydrogen gas. Connections concerned during the compression portion of the loading cycle are indicated by white circles.

29 August 2023 13:59:20

but no loss in lateral stiffness, which might affect the alignment of the test.

There are three seals in the top end cap (left yellow end cap in Fig. 3) on which the pull rod “rides.” The reason that there are three seals is to contain the gas in the main chamber and in the antechamber, which balances the axial load from the gas pressure. These seals are u-cup type seals, where gas pressure inside of the u-shape causes expansion, resulting in a seal. The seals are made of a polymer and, therefore, provide little lateral stiffness. While an alignment bearing attached to the inside of the end cap, close to the specimen grip, would be an ideal position to provide lateral stiffness to the load train, there is not sufficient space inside the vessel for such a bearing. Instead, an alignment bearing is attached to the end cap outside of the test vessel. This configuration is not as effective in providing lateral stiffness but nevertheless adds some needed lateral stiffness.

Inside the test vessel are the specimen, one or more extensometers, a load cell, and custom specimen grips. The load cell handles both compressive and tensile loads up to 44 kN (10 kips) and is designed for maximum lateral stiffness. The load cell, also a strain-gauge type, has a maximum uncertainty of 0.3%.

For our baseline measurements, we used a thick commercial gas cylinder that had been in hydrogen service and was certified for use up to 41 MPa (6000 psi) as our baseline material for strain-life testing. This cylinder was constructed from a 4130-grade pressure vessel steel. The cylinder had an outer diameter of 230 mm (9 in.) and a wall thickness of 16.5 mm (0.65 in.), which dictates how long the specimen can be and the maximum diameter of the button ends. The height of the cylinder was 1.3 m. We also investigated a couple of higher strength (UTS = 1040 and 1180 MPa) pressure vessel steels from experimental hydrogen cylinder designs, which had not seen service. The vessel with the thinnest walls, which used the 1180 MPa UTS steel, had an outer diameter of 230 mm and a wall thickness of 7.44 mm (0.3 in.).

As much as possible, we followed ASTM guidelines for sample design both for strain-life testing and for testing in hydrogen. However, we had to make some deviations from these recommendations due to constraints in the material available (especially due to the cylinder wall thickness) and our experimental setup within the hydrogen chamber. In the following, we discuss sample design and the considerations for which recommendations were followed, and when we had to deviate from the standards.

As we cut these samples from cylindrical materials, geometric constraints generally determine the maximum diameter for which a specimen can be made, with the thickness of the starting material and the radius of curvature of the starting material being the

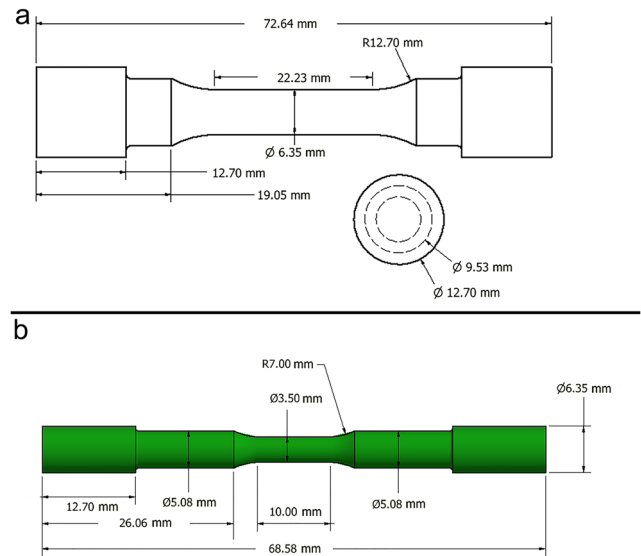


FIG. 5. Drawings of strain-life specimens for (a) baseline steel and (b) high-strength steel. The bottom specimen is sized in accordance with ASTM E606 but the top one is not, due to the need to test in the circumferential as well as the longitudinal direction for that material.

dominant geometric constraints. This is particularly true when specimens are needed in the circumferential (or transverse) direction, Fig. 4. From Fig. 4, it can be seen how specimen size must scale with wall thickness and cylinder diameter: a thinner wall or a small cylinder diameter necessarily leads to smaller specimen sizes.

The ASTM E606 standard allows for specimens with cylindrical geometry or hemispherically concave geometry.¹⁴ We used cylindrical geometry, which enables the use of a linear extensometer. Two specimen designs are shown in Fig. 5. The geometry of the specimens is measured to within a maximum uncertainty of 0.35%.

The ASTM E606 standard for strain-life testing has a recommended minimum specimen diameter in the gage section of 6.35 mm. For the baseline material, this was achieved, see Fig. 5(a). However, for the thin-walled vessel materials, it was not possible to meet this minimum gage section requirement within the geometric constraints of the specimen design. The steels used for these thin-walled vessels are of higher strength, which lowers the propensity for buckling. In addition, the ASTM E606 standard allows for other diameters and cross sections. For high-strength steels from pressure vessels (gas cylinders, in this case), gage sections with diameters as

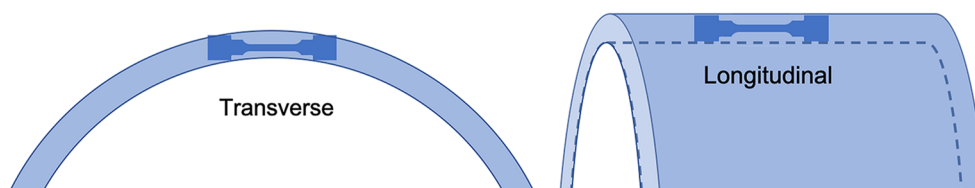


FIG. 4. Diagram showing how strain-life specimens are cut from a cylindrical material section such as a gas cylinder or pipeline in the transverse or circumferential direction and the longitudinal direction.

small as 3.5 mm were used, see Fig. 5(b). The part of the test section that is outside of the gage section is recommended to be twice the diameter of the gage section but can be less than that for materials that are typically ductile, such as pressure vessel steels and pipeline steels.

The ASTM E606 standard recommends that a specimen for strain-controlled fatigue testing be $20d \pm 4d$ long with a uniform gage section $3d \pm d$ long, where d is the diameter of the specimen gage section. It was necessary to measure in the circumferential direction and compare that to measurements in the longitudinal direction to determine whether the steel had significant anisotropy. Therefore, the specimens made [Fig. 5(a)] do not have a total length that corresponds to the ASTM E606 recommendations (they are $\sim 11d$), although the gage section is in accordance with recommended geometry ($3.5d$). Measurements on the higher-strength gas cylinder use specimens [Fig. 5(b)] where the lengths correspond to ASTM E606 recommendations, but the diameter of the gage length is only 3.5 mm due to the thin cylinder walls.

Specimens tested in hydrogen must have a fine surface finish because even marks left by machining that do not affect the lifetime in the air will often cause premature crack initiation in hydrogen environments. Therefore, the surface finish guidelines from ASTM G142 were followed, where polishing to a finish better than $0.25 \mu\text{m}$ is used.¹⁶ The specimens' gage sections were polished both longitudinally and transversely to provide a surface finish in accordance with ASTM G142. The shoulder sections were polished on a lathe with 600-grit emery paper to round that section slightly and to remove machine marks.

Both sample geometries provide reliable results in air and in pressurized hydrogen gas. However, the smaller (3.5 mm diameter) specimen design has a relatively small difference in diameters between the button head and the test section outside of the gage section. This small amount of material must withstand the forces of the test in both tension and compression. For measurements in air where the material retains its full ductility, the inner radius between the test section and the button head is sufficiently large that cracking does not occur there, but within the gage length. For tests run in pressurized hydrogen gas, as the material loses ductility, this inner radius is subject to premature cracking. This is usually due either to the relative sharpness of this transition, or due to machining marks, which are difficult for a machinist to avoid. By polishing this radius manually with 600-grit emery cloth, the number of successful tests in hydrogen gas increased.

To hold the button-head ends of our specimens, we use a custom collet-type design, see Fig. 6. This is not uncommon for strain-life testing, but our design uses materials that perform well in hydrogen environments. The collets are made of maraging C250 steel (in annealed condition) and the grip bodies and bolts are made of A286 stainless steel. The button heads of the specimens are compressively loaded by bolts in the grips to hold them tight against counterfaces up to tensile and compressive loads of 24 kN (5.5 kips). The loading of the bolts takes place with the assembly (specimen, both sets of grips, and both pull rods) mounted in a lathe. The bolts are tightened progressively such that a consistent gap is maintained at each fixture and around the circumference of each custom grip. During this loading, the specimen is centered with respect to the grips, accounting for the linearity, eccentricity, and perpendicularity of the whole assembly.

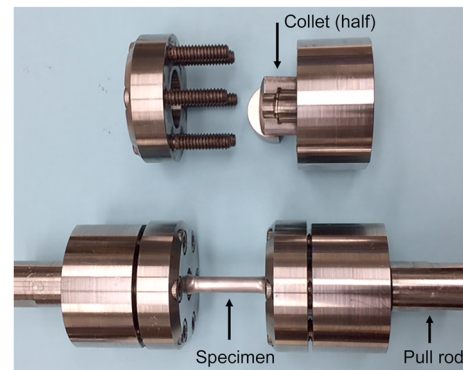


FIG. 6. Picture of the sample grip assembly. Top shows disassembled grip with half of a collet in place. Two collet halves fit around the sample button head, which is compressively loaded in the grip by bolts. Bottom shows fully assembled grips with the specimen in the center, and upper and lower pull rods attached.

The lateral rigidity and linear alignment of all the components within the test chamber must be maintained, including specimen, holding fixtures, load cell, and pull rod. The lower section comprising a lower end cap, load cell, and specimen/grip fixture (described in the previous paragraph) forms one rigid segment when assembled. The pull rod, compression clevis, and actuator of the load frame form a second upper rigid segment.

Alignment of all components to the actuator of the load frame is crucial for fully reversed loading. The large compressive loads seen during these tests, over 20 kN in some cases, can cause bending of the specimen if the equipment is not properly aligned. The parameters measured and derived for strain-life will also be inaccurate if the loading includes appreciable bending stresses. Two methods were used to measure alignment: a strain-gauged specimen, and the use of two calibrated extensometers set at various positions and at either 90° or 120° offsets. We were able to achieve alignment of better than 1% of the maximum axial strain range, while the standard calls for alignment of better than 5% of the maximum axial strain range. The two-calibrated-extensometers method became our default arrangement for testing. It is worth noting that the strain-gauge-type extensometers used in this work have a maximum uncertainty of 0.25%. In more recent tests, a third method has been added: a digital camera is attached to the inside of the pressure vessel, allowing for visual examination of the alignment from assembly throughout the duration of the test, and providing a third in-test verification of alignment.

The two extensometers are attached to the specimen by using elastic bands or springs. They are placed 90° – 120° apart, which provides information on sample bending during a test: when bending occurs, the two extensometer readings begin to deviate from each other. The load cell and extensometers are both custom designs and use strain gauges that have been shown to work well in an environment of pressurized hydrogen gas.^{17,18} The strain gauges were “C” shape in design. The measurement length of the strain gauges was selected to match the sample geometry, with the larger specimens measured using 19 mm (0.75 in.) gage length extensometers and the smaller specimens using 8 mm gage length. The extensometers were calibrated with a strain range of ± 0.1 strain.

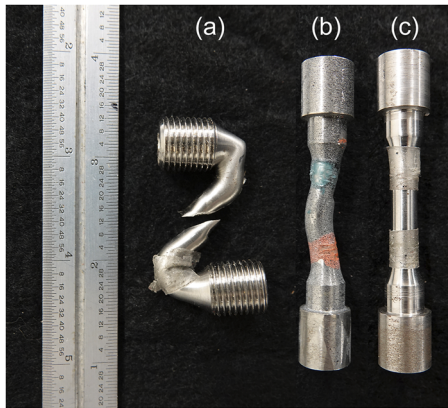


FIG. 7. Specimens tested under strain control where the alignment and control gain were not correct (a), the control parameters were correct, but the alignment was not adequate (b), and both control and alignment were both adequate (c). (Note: colored or taped regions are to aid in strain-gauge gripping of the sample surface without damaging the surface finish.)

Misalignment, even small misalignment, or incorrect control parameters can affect strain-life tests. A strain-life test relies on an extensometer mounted to the specimen, usually with knife edges and a spring or elastic band to keep the knife edges of the extensometer from slipping. Slipping of the extensometer can result in very rapid and large movements of the actuator, which will invalidate a test. Incorrect control parameters such as having too much gain can also cause rapid actuator movements, which can cause slippage of the extensometer and further large and rapid actuator movements. This will invalidate a test and typically destroy the specimen. For instance, Fig. 7(a) shows a specimen where the alignment was not adequate and the control had too much gain. The extensometer subsequently slipped, and this continued to get worse until the extensometer fell off, which resulted in a twisted and sheared-off specimen. When the control parameters are correct but alignment is not adequate, the specimen will bend in the shape seen in Fig. 7(b). When the alignment and control parameters are adequate, the specimen will remain straight, despite the compressive loads, as in shown Fig. 7(c). Note that the setup evolved from threaded specimens [Fig. 7(a)] to custom button-headed specimens [Figs. 7(b) and 7(c)], which decreases the overall system compliance. As mentioned earlier, testing in accordance with ASTM G142 requires polishing of the gage section of the specimen, which makes slippage of the knife edges of the extensometer more likely. The use of nail polish and/or double-stick tape to create a surface to which the knife edges can stick solves this issue while minimizing scratching.

VALIDATING THE DATA

Due to the entire apparatus necessarily being reassembled and disassembled for each test, there is the possibility to introduce misalignments into any given test. Consequently, each test is validated by observing the test, checking the samples for bending after each test, and analyzing the test data. This section covers the process undertaken to validate each test. It should be noted that approximately one in five tests of the baseline (thicker) specimen geometry

fail validation and are not included in our datasets. For the thinner specimens, where the margin of error for alignment is smaller, the failure rate is greater, with less than half of the tests being considered valid. Due to the presence of the hydrogen chamber, none of the tests in hydrogen gas fully comply with ASME E606, although its procedure was followed or approximated as closely as possible.

As mentioned previously, two extensometers mounted $\sim 120^\circ$ apart were used for each test. Comparing the two extensometers allows bending of the sample to be observed in most cases. On a properly aligned test, such as the example shown in Fig. 8(a), the hysteresis curves from each extensometer are rotationally symmetric and the data for the two extensometers match quite closely. In the figure, the data from early in the test (cycle 2) from the controlling extensometer (1) is shown as black squares, with the filled shapes showing the tension portion of the hysteresis curve and the open squares showing the compression portion of the curve. The two portions of the curve match well. Due to it being the controlling extensometer, the data are quite smooth. The second/observing extensometer data are shown as blue circles (again, filled are tension and open are the compression data). In this test, the second extensometer shows a bit of noise, but the hysteresis curve is symmetric and matches the controlling extensometer data closely.

At the midpoint, or stabilized cycle, of the test (616 cycles for this particular test), the same trends can be seen. The controlling extensometer data (red triangles) are symmetric and smooth. Due to this material showing softening behavior, the maximum stress is lower than in cycle 2, as expected. The data from extensometer 2 match extensometer 1 better than earlier in the test, and the data are smoother. Throughout the test, until cracking occurs, the maximum strains measured by each extensometer are well within the 5% required by ASME E606, with an average difference between the extensometers of 1%.

For comparison, a cycle shortly before final failure, after a crack has initiated and is starting to grow, is shown. Only extensometer 1 is shown, as the data for extensometer 2 was essentially just noise due to the position of the crack. For the tension portion of the curve (filled navy stars), the maximum stress/force is falling rapidly due to the crack reducing the load-carrying cross-sectional area of the sample. In compression, the crack is closed and the load-carrying cross-sectional area is virtually identical, resulting in a similar maximum compressional stress/force as in the stabilized/half-life cycle.

For a misaligned test, the data look quite different, see Fig. 8(b). The data shown are for the same sample geometry, same material, and same applied strain amplitude as for the properly aligned test in Fig. 8(a). The data from extensometer 1 of cycle 2 are again shown in black squares (filled for tension and open for compression). The hysteresis curve appears symmetric. The curve is also very similar to that of the aligned test, with a similar maximum stress (~ 600 MPa) upon reaching the maximum strain amplitude (0.0046). However, the data from extensometer 2 (blue circles) are quite different due to the misalignment. While similar maximum stresses are reached in tension and compression, the curve is clearly not rotationally symmetric about the origin due to the bending of the sample. This is still evident at cycle 616, where the controlling extensometer data are symmetric but extensometer 2 data are not. The difference in the maximum strains between the two extensometers generally

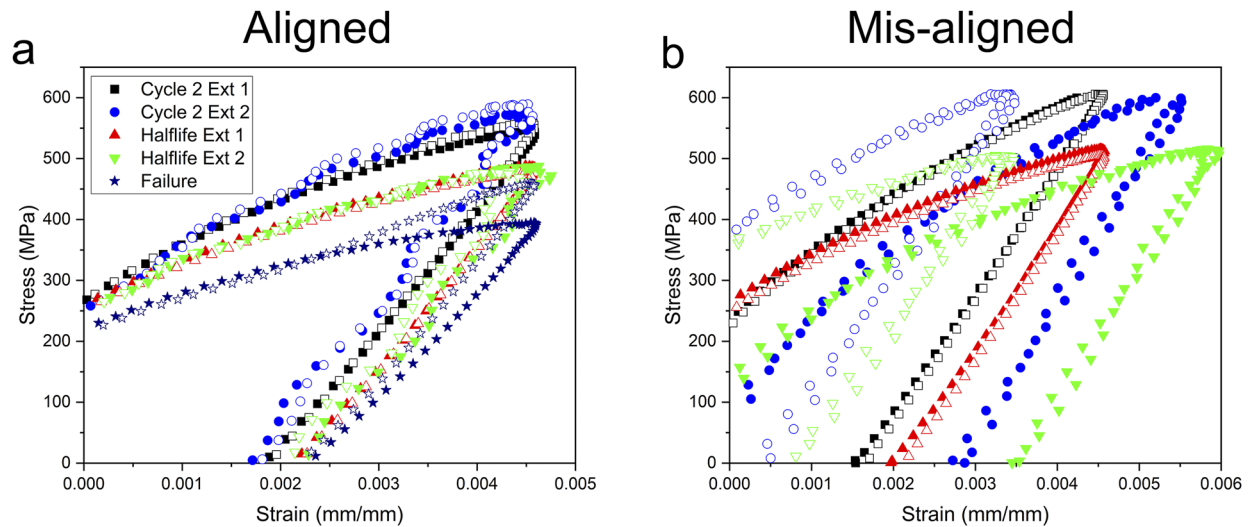


FIG. 8. Comparison of the data from two extensometers on (a) an aligned and (b) a misaligned test. Both tests were run on the same baseline material in the same specimen geometry and were run at the same strain amplitude ($\epsilon_a = 0.0046$). Filled symbols indicate the tension portion of the hysteresis curve (positive stress and strain), and open symbols indicate the compression portion of the hysteresis curve (negative stress and strain, absolute values shown here to compare the symmetry of the hysteresis curve). Extensometer 1 (Ext 1) is the controlling extensometer. Extensometer 2 (Ext 2) is a second extensometer attached $\sim 120^\circ$ from the controlling extensometer on the sample gage section. Note that in the aligned test, the hysteresis curves for both extensometers lined up well and are symmetric (tension and compression nearly identical), while in the misaligned test, extensometer 2 displays asymmetry. The degree of bending (difference between the extensometers) is around 1% in the aligned test and around 29% in the misaligned test.

remains at around 29% throughout the test, giving the degree of bending with each cycle. This sample was not pulled to failure due to the evident bending occurring.

Samples from early tests where a crack was not generated were examined in a lathe to determine whether the sample bent or not during testing. Some samples, as shown in Fig. 7(b), show evident bending without the need of spinning the samples. Some samples are less evident by eye but display noticeable eccentricity when spun in a lathe. Bent samples correlate with the tests that showed asymmetrical data.

Samples were also examined after testing to determine the position of the crack relative to the extensometers. (If possible, tests were stopped after “failure,” drop of 50% of the maximum load, but before the final separation of the sample, in order to protect the equipment, such as the extensometers.) In the hydrogen environment, it is not uncommon for stress risers, such as the point where the shoulder meets the button head or large machining marks, to be the initial point for failure, rather than cracks initiating due to the strain damage between the extensometers. Tests, where the crack was found outside of the extensometer gage section, were deemed invalid.

If the data showed good alignment of the sample, and cracking occurred within the valid portion of the gage section, the test was considered valid, and the data were analyzed as described in the next section.

TEST RESULTS

Fully reversed strain-life tests were conducted on 4130 pressure vessel (martensitic/ferritic—quench and tempered) steel which had

a 0.2% offset yield strength of 696 ± 17 MPa and an ultimate tensile strength of 793 ± 12 MPa. Tests were conducted in hydrogen gas at a pressure of 18 MPa. A typical stress-strain curve from the stabilized cycle of a strain-life test is shown in Fig. 9(a). The hysteresis curve endpoints and the points where the curve crosses the stress axis are used in the analysis of the data to determine total strain and to separate elastic and plastic contributions to the total strain, respectively.

The hysteresis curves themselves also indicate the quality of the test. A rotationally symmetric hysteresis curve is indicative of good alignment. Misalignments will be evident by a lack of symmetry. This is even evident in a well-run test: after a crack has initiated, the curve becomes asymmetric as the area of the cracked sample becomes smaller, reducing the amount of load that can be held in tension, yet in compression, the sample can still maintain the maximum load across the entire cross-section.¹

As the strain-life measurement cycles progress, the material can soften, harden, or stay stable depending upon the composition of the material and the microstructure of the material. In this case, the pressure vessel steel softens during cyclic loading, see Fig. 9(b). This plot captures the drop in the ends of the hysteresis curves, such as the one shown in Fig. 1(a). Since this is quench-and-temper steel, the amount of cyclic softening, or even whether it softens, can change based on the amount of tempering and the conditions of quenching.

One way to present the data from strain-life testing is to use the endpoints of the stabilized hysteresis loops from tests completed at various strain amplitudes and construct a stress-strain response plot, see Fig. 9(c). Note how the maximum and minimum stresses increase in magnitude as the strain amplitude increases but not linearly. This behavior shows similarities to a monotonic stress

strain curve where, after a linear elastic region, the curve bends over as plasticity occurs. In this case, the degree of softening or hardening of the material will determine the shape of the curve. This curve can be fit to a Ramberg–Osgood relation: $\epsilon_a = \frac{\sigma_a}{E} + \left(\frac{\sigma_a}{K'}\right)^{1/n'}$, where ϵ_a is the strain amplitude, σ_a is the stress amplitude, E is the elastic modulus, and K' and n' are fitting parameters. This curve, once fit to several stabilized hysteresis curves, can be used to predict the stabilized response at other strain amplitudes.²⁰ Different materials will show variations in this response. In addition, comparisons between the curves of the same material produced under different conditions, such as in-air and in-hydrogen, can give information on the effect of the environment, for example, on the softening or hardening behavior of the material.

The most common way to present strain-life data is to use a lifetime plot, see Fig. 9(d). This shows lifetime in the form of strain amplitude as a function of cycles. Data covering multiple decades of lifetime are often used for materials selection and part design. As we are not certifying materials, we focused on acquiring several data points around each of four decades of lifetime (10, 100, 1000, and 10 000 cycles). The curve fitted to air data produced with the same material¹⁹ is plotted for reference, and it is immediately clear that hydrogen causes an order of magnitude drop in lifetime under similar loading conditions. The data are plotted for total strain and separated into the elastic and plastic components. The separation of the total strain into elastic and plastic components is done by analyzing the stabilized cycle [see Fig. 9(a)] to determine

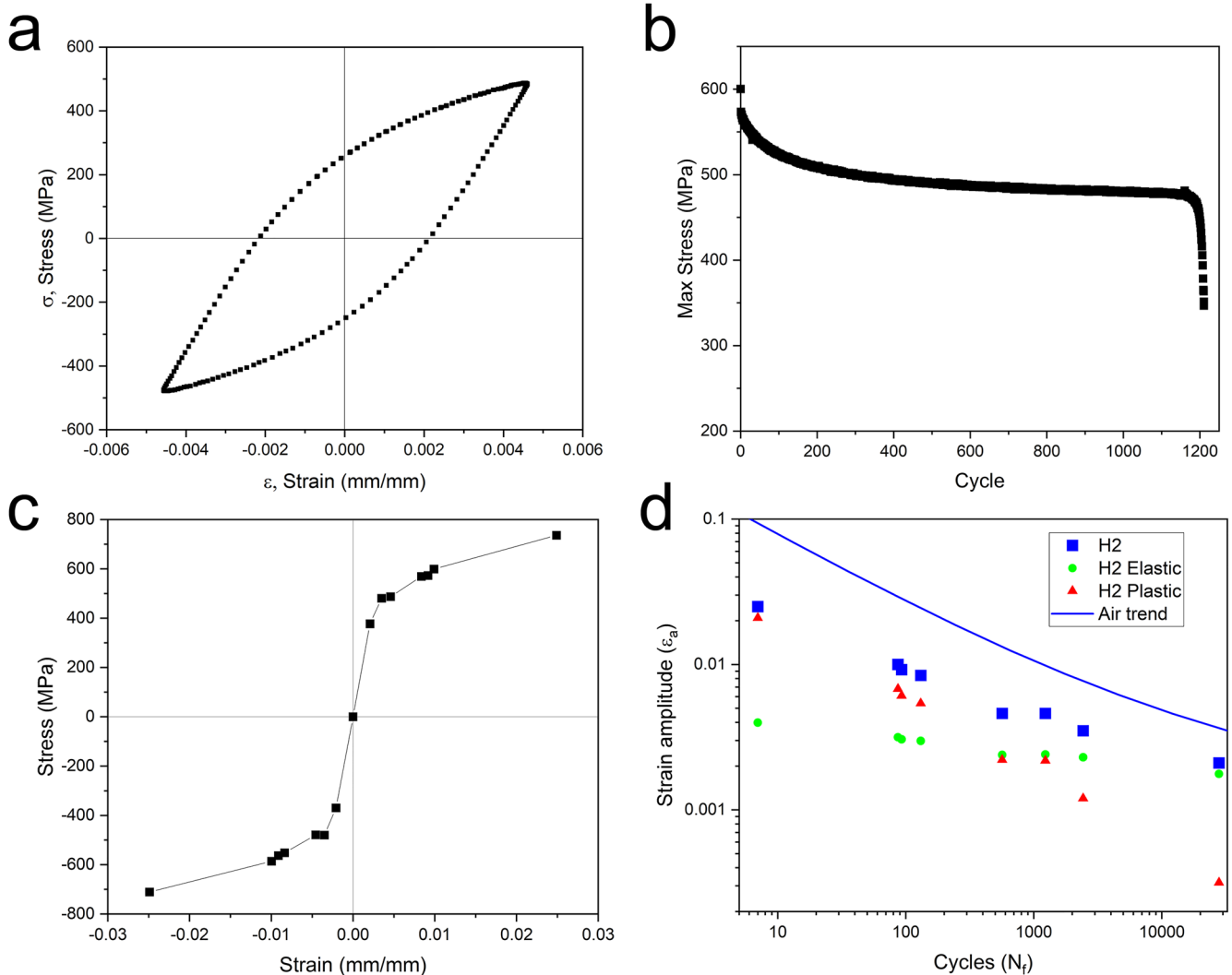


FIG. 9. (a) Stabilized hysteresis loop of stress as a function of strain for measurement of strain-life of baseline material (4130 pressure vessel steel) at a strain amplitude of 0.0092 and a hydrogen gas pressure of 18 MPa. (b) Plot of stress as a function of cycles at a strain amplitude of 0.0046 and a hydrogen gas pressure of 18 MPa. At this condition, the lifetime was 1210 cycles. (c) Cyclic stress–strain curve: stress–strain response plot from stabilized hysteresis loops of strain-life tests at varying strain amplitudes. (d) Lifetime plot of hydrogen strain-life data given as total strain and separated into elastic and plastic components. The total strain-life data trend for measurements run in the air is shown for comparison.¹⁹

the relative proportions of the linear and non-linear portions of the curve.²¹ The elastic and plastic components tend to follow relationships that are linear on a logarithmic plot. Comparing the elastic and plastic components can be useful because there are cases where material response as total strain is similar but significant differences are found in either the elastic or plastic components, or both.^{1,2}

Comparison with the air data also gives confidence in the accuracy of the in-hydrogen data. The stabilized hysteresis curves at the same strain amplitude were found to be very similar in air and in hydrogen. The largest difference is that the maximum stress varies slightly due to differences in softening, which is reasonable, given the known effects of hydrogen on dislocation activity.^{22,23} This results in the overall cyclic stress–strain curve in hydrogen [Fig. 9(c)], and in-air, shown in Ref. 24, being very similar: both follow Ramberg–Osgood relationships but with a slight difference in the height of the curve. These differences due to hydrogen will be the subject of further study.

With these data, further analysis can be done, such as comparing softening curves [Fig. 9(b)] as a function of strain amplitude and environment or comparing the partitioning of elastic and plastic strain amplitude between different materials. In addition, this rich dataset is useful for modeling damage to predict failure, as the quantification of elastic and plastic components can elucidate path-dependent deformation and damage accumulation during loading. While some of this analysis can be found in another publication,²⁴ further analysis of the data will be the subject of future papers.

CONCLUSIONS

Alterations were necessary to adapt current capabilities for fatigue crack growth rate and tensile testing in a high-pressure hydrogen environment to fully reversed strain-controlled fatigue testing—strain-life testing. This included developing new sample-gripping fixtures and a specially developed “compression clevis” to ensure that the ASTM requirements for strain-life testing were met as closely as possible. Samples were designed that met as many of the ASTM requirements as possible, given the constraints of the parent material from which samples were extracted. The stringent size limitations from ASTM on the sample dimensions may be difficult to meet in newer high-strength (thin-walled) materials in general, but our results suggest that slight variations may still provide valid and useful data. Valid strain-life tests on a baseline material in the hydrogen environment have been successfully conducted according to the ASTM requirements, and the results promise interesting insights into the hydrogen effects on this material’s mechanical response.

ACKNOWLEDGMENTS

This work was funded by NIST and the U.S. Department of Transportation Project No. DTPH5615X00015.

AUTHOR DECLARATIONS

Conflict of Interest

The authors have no conflicts to disclose.

Author Contributions

P. E. Bradley: Investigation (equal); Methodology (equal). **M. L. Martin:** Visualization (equal); Writing – original draft (equal). **M. J. Connolly:** Investigation (equal). **R. L. Amaro:** Conceptualization (lead); Formal analysis (lead). **D. S. Lauria:** Data curation (lead); Investigation (equal); Software (lead). **A. J. Slifka:** Investigation (equal); Project administration (lead); Resources (lead); Writing – original draft (supporting).

DATA AVAILABILITY

The data that support the findings of this study are available from the corresponding author upon request.

REFERENCES

- 1 J. Bannantine, J. Comer, and J. Handrock, *Fundamentals of Metal Fatigue Analysis* (Prentice Hall, Englewood Cliffs, NJ, 1990).
- 2 S. Suresh, *Fatigue of Materials*, 2nd ed. (Cambridge University Press, 2004).
- 3 Y. Murakami and H. Matsunaga, *Int. J. Fatigue* **28**(11), 1509 (2006).
- 4 G. Schauer, J. Roetting, M. Hahn, S. Schreijae, M. Bacher-Höchst, and S. Weihe, *Procedia Eng.* **133**, 362 (2015).
- 5 P. S. Lam, R. L. Sindelar, A. J. Duncan, and T. M. Adams, *J. Pressure Vessel Technol.* **131**(4), 041408 (2009).
- 6 H. Barthélémy, *Int. J. Hydrogen Energy* **36**(3), 2750 (2011).
- 7 J. A. Ronevich, B. P. Somerday, and C. W. San Marchi, *Int. J. Fatigue* **82**, 497 (2016).
- 8 C. San Marchi, B. P. Somerday, K. A. Nibur, D. G. Stalheim, T. Boggess, and S. Jansto, *ASME 2010 Pressure Vessels and Piping Division/K-PVP Conference*, (ASME, 2010), p. 939.
- 9 Z. S. Hosseini, M. Dadfarnia, A. Nagao, M. Kubota, B. P. Somerday, R. O. Ritchie, and P. Sofronis, *J. Appl. Mech.* **88**(3), 031001 (2020).
- 10 N. E. Nanninga, Y. S. Levy, E. S. Drexler, R. T. Condon, A. E. Stevenson, and A. J. Slifka, *Corros. Sci.* **59**, 1 (2012).
- 11 M. L. Martin, M. Connolly, Z. N. Buck, P. E. Bradley, D. Lauria, and A. J. Slifka, *J. Nat. Gas Sci. Eng.* **101**, 104529 (2022).
- 12 A. J. Slifka, E. S. Drexler, R. L. Amaro, L. E. Hayden, D. G. Stalheim, D. S. Lauria, and N. W. Hrabe, *J. Pressure Vessel Technol.* **140**(1), 011407 (2017).
- 13 A. J. Slifka, E. S. Drexler, N. E. Nanninga, Y. S. Levy, J. D. McColskey, R. L. Amaro, and A. E. Stevenson, *Corros. Sci.* **78**, 313 (2014).
- 14 ASTM, ASTM E606 ASTM Standard: Standard test method for strain-controlled fatigue testing (2020).
- 15 H. J. Cialone and J. H. Holbrook, *J. Metall. Trans. A* **16**(1), 115 (1985).
- 16 ASTM, ASTM standard: Standard test method for determination of susceptibility of metals to embrittlement in hydrogen containing environments at high pressure, high temperature, or both (2016).
- 17 R. Tobler and J. Shepic, *J. Test. Eval.* **13**(4), 299 (1985).
- 18 R. J. Billia, Strain gages subjected to a high pressure hydrogen environment (1975).
- 19 C. P. Looney, Z. M. Hagan, M. J. Connolly, P. E. Bradley, A. J. Slifka, and R. L. Amaro, *Int. J. Fatigue* **132**, 105339 (2020).
- 20 G. Zonfrillo and D. Nappini, *J. Mech. Eng. Autom.* **5**, 362 (2015).
- 21 N. E. Dowling, *Fatigue Fract. Eng. Mater. Struct.* **32**(12), 1004 (2009).
- 22 M. L. Martin, M. Dadfarnia, A. Nagao, S. Wang, and P. Sofronis, *Acta Mater.* **165**, 734 (2019).
- 23 K. M. Bertsch, S. Wang, A. Nagao, and I. M. Robertson, *Mater. Sci. Eng.: A* **760**, 58 (2019).
- 24 M. L. Martin, P. E. Bradley, D. Lauria, R. L. Amaro, M. Connolly, and A. J. Slifka, *ASME 2022 Pressure Vessels & Piping Conference* (ASME, 2022).